Smart Structures and Systems, *Vol. 15, No. 3 (2015) 683-698*
DOI: http://dx.doi.org/10.12989/sss.2015.15.3.683

System identification of an in-service railroad bridge using wireless smart sensors

Robin E. Kim*, Fernando Moreu[a] and Billie F. Spencer, Jr.[b]

Department of Civil and Environmental Engineering,
University of Illinois at Urbana-Champaign, Urbana, IL 61801, USA

(Received November 27, 2014, Revised February 10, 2015, Accepted February 15, 2015)

Abstract. Railroad bridges form an integral part of railway infrastructure throughout the world. To accommodate increased axel loads, train speeds, and greater volumes of freight traffic, in the presence of changing structural conditions, the load carrying capacity and serviceability of existing bridges must be assessed. One way is through system identification of in-service railroad bridges. To dates, numerous researchers have reported system identification studies with a large portion of their applications being highway bridges. Moreover, most of those models are calibrated at global level, while only a few studies applications have used globally and locally calibrated model. To reach the global and local calibration, both ambient vibration tests and controlled tests need to be performed. Thus, an approach for system identification of a railroad bridge that can be used to assess the bridge in global and local sense is needed. This study presents system identification of a railroad bridge using free vibration data. Wireless smart sensors are employed and provided a portable way to collect data that is then used to determine bridge frequencies and mode shapes. Subsequently, a calibrated finite element model of the bridge provides global and local information of the bridge. The ability of the model to simulate local responses is validated by comparing predicted and measured strain in one of the diagonal members of the truss. This research demonstrates the potential of using measured field data to perform model calibration in a simple and practical manner that will lead to better understanding the state of railroad bridges.

Keywords: calibrated numerical model; structural health monitoring system; railroad bridge; system identification; wireless smart sensors

1. Introduction

Railroads have been an important part of the transportation network for over a hundred years in the United States (US).The freight rail industry has been the fastest growing segment since 1980, accounting approximately 40 percent of the total freight moved nationwide in 2010 (FRA, 2010). Due to continuous growth in freight demand, the Association of American Railroad forecasts that rail lines exceeding their capacity will increase from 173.81 km (108 miles) to nearly 25,749 km (16,000 miles; AAR, 2012).In an effort to meet the expected increase in the demand, the private

*Corresponding author, Ph.D. Candidate, E-mail: kim491@illinois.edu
[a] Ph.D. Candidate, Email:moreualo@illinois.edu
[b] Professor, Email: bfs@illinois.edu

http://www.techno-press.org/?journal=sss&subpage=8 ISSN: 1738-1584 (Print), 1738-1991 (Online)

US freight railroads have been emphasizing maintenance of their infrastructure, by organizing the majority of their revenue to ensure or to maintain the good state of their network. To date, as much as 15 to 20 percent of their total capital is used to enhance/maintain the railroad capacity (FRA, 2010). Thus, researches that can appropriately assess such infrastructure are assuming greater importance.

Amongst railroad networks, bridges form a critical link. According to the FRA documents in 2002, the US railroad network contained an average of one bridge for every 2.25 km (1.4 miles) of track (GAO, 2007). Ensuring good conditions for those bridges is important because they are the most expensive pieces of railroad networks; replacement and construction cost of railroad bridges can be 11 to 550 times as much per linear foot as regular track (GAO, 2007). At the same time, those structures are susceptible for severe wear or deterioration when the structures age and serve heavier traffic than their original design to meet the increased demands. Methods for quickly assessing physical states of the railroad bridges whether they can accommodate increased axle loads, train speeds, and greater volumes of freight traffic became of primary needs for railroad engineers (Moreu and LaFave 2012).

Numerous researchers have employed system identification to develop models of highway bridges that can help in assessing the state of bridge infrastructure. Because initial models for the bridge may not be 100% successful for assessing dynamic properties, models are usually updated using measurements from dynamic testing. Various model updating approaches have been proposed (e.g., Brownjohn and Xia 2000, Jaishi and Ren 2005, Deng and Cai 2009, Morassi and Tonon 2008). While aforementioned literature used models that well represent global features of the bridge, Catbas *et al*. (2007) asserted that for accurate and practical condition evaluation of a structure, models should not only be updated with global attributes, but also with local data; when local responses are estimated from global-only calibrated model, results may be render meaningless. As such, in some of applications, global responses are measured from ambient vibration tests using accelerometers. Then, local characteristics, such as strain, are captured from controlled tests; the bridge is usually closed for the revenue traffic while a truck of known mass runs over the bridge (Catbas *et al*. 2008, Brenner *et al*. 2010). Although this type of test strategies is relatively easy to achieve in highway bridges, in the case of railroad bridges, performing such tests can be much expensive and hard. In consequence, railroad bridges received comparably less attention in this topic. Thus, a framework for monitoring railroad bridges that can efficiently reach global and local calibration of a model for system identification under revenue traffic needs to be devised.

To date, only a limited number of studies have conducted system identification of in-service railroad bridges. Ahmadi and Daneshjoo (2012) implemented a full-scale monitoring system on a railroad bridge (Firoozeh Railroad Bridge, Iran). They collected acceleration responses of the bridge under a train of known speed and weight passing and extracted key parameters of the bridge. Giles *et al*. (2011, 2012) implemented a full-scale monitoring system on the Government Bridge at the Rock Island Arsenal using wireless smart sensors (WSSs). The efficient and multi-metric system allowed understanding of the global behavior of the bridge (Cho *et al*. 2014). Local responses are also measured from fiber optic strain sensors. However those sensors were only suitable for static measurements, because of the aliasing effects (Van Damme *et al*. 2007). In their application, however, because the bridge could swing to allow river traffic (i.e., barges) to pass, and thus traffics are closed and static loads governed during the period, use of those sensors were adequate. From the member strain under self-weight, the health of the bridge was assessed. In addition, system identification of the bridge was performed comparing global responses of the bridge with a finite element (FE) model (Cho *et al*. 2014). While these methods have been successful in monitoring railroad bridges, a framework for dynamic tests and calibrated models that can help practically assess in-service railroad bridges based on global and local responses has not been provided.

This paper demonstrates the use of measured data to identify a railroad bridge and calibrate an FE model to understand the global and local behavior of an in-service railroad bridge. This effort includes three distinct phases: (i) selection of a railroad bridge and implementation of a monitoring system with WSSs; (ii) an FE model development based on original construction design; and (iii) model calibration and validation using global and local responses of the bridge. In the monitoring system, WSS networks were installed on a steel truss railroad bridges. An FE model is developed and updated with field measurements so that the model can well represent the bridge both globally and locally. The results of this study demonstrate a framework, which can be used for understanding an in-service railroad bridges under revenue traffic to help railroad engineers managing their bridges.

2. Description of test bridge and monitoring system

A structural health monitoring (SHM) system was installed on a railroad bridge owned by Canadian National Railway (CN). The system comprised a set of WSSs, which provide services suitable for efficient monitoring system. During the research period, the system was able to collect various measurements. The uniqueness of the test bridge enabled rich collection of the measurements. This section demonstrates a successful layout of the system and examples of field data.

2.1Test bridge

A railroad bridge located over the Little Calumet River near Chicago, IL (see Fig. 1) has been selected in this study for assessing its structural conditions. Among the four bridges shown in the Fig. 1, the instrumented bridge is an intermediate truss bridge (the bridge with an arrow); the West-most bridge in the Fig. 1 is the Metra lane, another truss bridge carrying freight and passenger trains located the East to the test bridge, the East-most bridge is closed for the traffic. The bridge is about 95 m long, 21 m tall, and 10 m wide steel bridge and made of A36 American Society for Testing and Materials (ASTM).The bridge opened for service in 1971, with an expected life of 100 years. The test bridge carries two tracks, CN1 track on the West side and CN2 track on the East side, which both are open for South and North bound freight and passenger trains. About ten freight trains and six Amtrak trains run on either CN1 or CN2 track in a daily basis. Those characteristics of the bridge make the bridge suitable and unique for the test bridge;(i) the test bridge is made of steel, which is the most common type in the US (53% of entire railroad bridge inventory, FRA, 2008); (ii) adjacent bridges are open to the traffic exciting the test bridge without changing mass of the bridge by carrying the train loads; and (iii) high traffic with various types of trains on the test bridge allows rich data collection from the monitoring system.

2.2 Monitoring system

WSS networks implemented on the bridge aimed for an efficient SHM system with various types of sensors. A wireless platform used in this project is an Imote2 platform (Crossbow Technology, 2009). This platform can stack a sensor board via two external connectors allowing flexible design of the network with any types of sensor boards. Sensor boards used in this project are (i) normal accelerometer board (herein, a set of this sensor board and the Imote2 will be noted as ISM400 sensor; (ii) high sensitivity accelerometer board (denoted as SHM-H sensor); and (iii) strain sensor (denoted as SHM-S sensor). Measurable range for an ISM400 sensor is up to ±2 g, while a SHM-H sensor can provide ten times higher sensitivity (i.e., up to ±200 mg). Each sensor node is equipped with a solar panel and rechargeable battery for energy harvesting. The essential driver and software for monitoring, such as synchronization and sensing are implemented, adopting services from Illinois Structural Health Monitoring Project (ISHMP) Services Tool suite (Rice *et al*. 2010, Jo *et al*. 2011).

Fig. 2 shows the WSS network map used in this paper. Components of the network are listed below with each of their objectives.

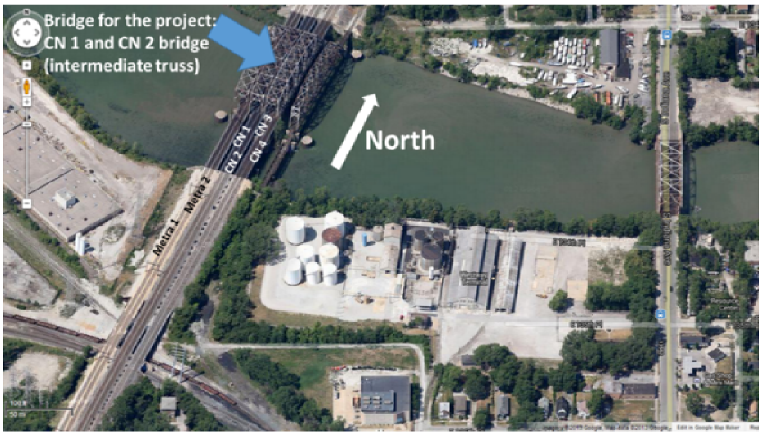

Fig. 1 Selected test bridge, near Chicago, IL*

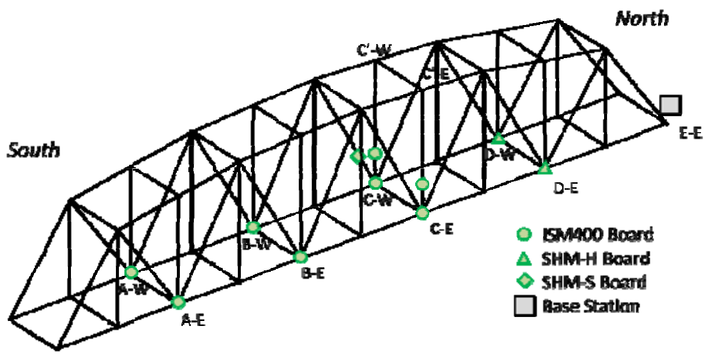

Fig. 2 WSS deployment map on the Calumet Bridge

*Google Maps (2014), www.maps.google.com.

- Six ISM400 sensors at A-E, A-W, B-E, B-W, C-E, and C-W.
- Two ISM400 sensors on 2.1 m higher locations from C-E and C-W, to eliminate the spatial aliasing and to captures way behavior of the bridge.
- Two SHM-H sensors at D-E and D-W to enhance the quality of the network effectively, while keeping total cost of the system low (Jo *et al*. 2012).
- One SHM-S sensor on a diagonal member of the bridge to provide local responses of the bridge. It was placed about 1.2 m South from C-Win Fig. 2. This member was chosen because of its uniqueness; the member experiences both tension and compression as the train passes the bridge.

In the final design of the network, two subnets were prepared; one for acceleration sensor nodes and the other for the strain sensor node. All acceleration sensor nodes were placed symmetrically in longitudinal direction (i.e., East and West), to allow obtaining asymmetric behavior under train loading on one side of the track. Those nodes were synchronized and provided synchronized responses with in a subnet of the truss bridge, which is then used for understanding the global behavior of the bridge. SHM-S sensor measured local responses of the bridge. Other than listed above and shown in Fig. 2, several SHM-S sensors were deployed on the rails both outside and inside the bridge as well. The sensors measured the train wheel loads, but the scope of this study will only cover the measurements from the structure. Finally, a base station PC, located at the North of the bridge (E-E in Fig. 2) controlled and collected data measured from two WSS networks (acceleration sensor network and strain sensor network). Having only 11 sensors, the system realized efficient and cost effective WSS networks tailored to monitor the global and local responses of the bridge under the train traffic.

2.3 Example of measured data

The measurements from the monitoring system under various train traffic formed a database for system identification. Fig. 3 shows an example of the acceleration response of the bridge when northbound Amtrak was passing the bridge on CN1 track at over 80 km/h. On each plot, the first vertical dashed line around 180 seconds indicates when Amtrak is entering the bridge, while the second vertical line near 190 seconds denotes exiting the bridge. As Amtrak passes the bridge, the bridge is excited laterally and vertically at similar degree (±15 mg). However, relatively small accelerations in longitudinal direction inform that Amtrak did not experience much change in acceleration (e.g., neither accelerating nor breaking). Because Amtrak is light and fast, the response of the bridge is similar that under impact tests. The transient responses after Amtrak left the bridge can give rich information of the global characteristics of the bridge.

3. System identification

This section explains the peak-picking method, an output-only system identification method. This method has been chosen due to its advantages over other methods for being fast, simple, and straight forward to extract key features of a structure. The accuracy of the selected method is shown as well, by comparing the results with Natural Excitation Eigensystem Realization Algorithm (NExT ERA).

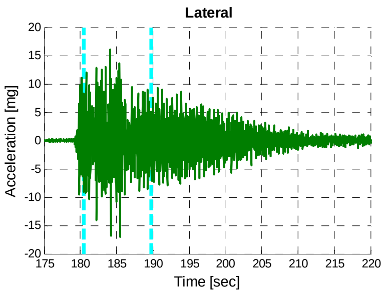

(a) Lateral acceleration.

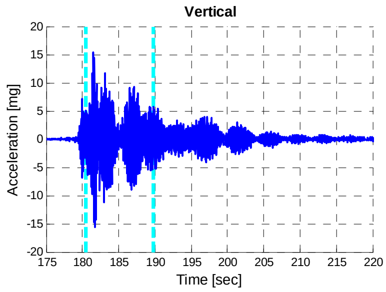

(b) Vertical acceleration.

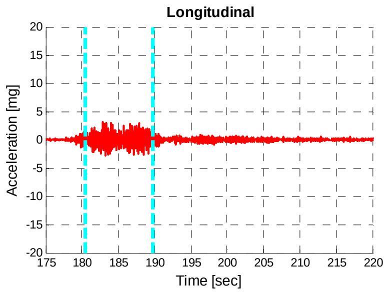

(c) Longitudinal acceleration.

Fig. 3 Bridge responses under northbound Amtrak on CN1 track measured at A-W (located near CN1 track)

3.1 Output-only system ID

In civil engineering structures, measuring input to the structure is difficult in most cases; hence, the modal parameters can identified from output-only system identification. A number of researchers provided frequency domain approaches to estimate the natural frequencies and mode shapes of the structure reasonably. Some widely used techniques are the frequency domain decomposition (FDD), Eigensystem Realization Algorithm (ERA), and peak-picking methods (Brincker *et al*. 2001, Juang and Pappa 1985, Brownjohn 2003). The expansion of those techniques uses acceleration measurement due to the ease of measuring acceleration rather than velocity and displacement of the structure. Among those, the peak-picking method is one of the simplest and fastest implementation for ambient vibration response (Brincker *et al*. 2001).

Felber (1993) introduced the peak-picking method for reliable estimation of modal frequencies and mode shapes for ambient vibration measurements. The basic theory of this method is that the frequency response goes to an extreme around the fundamental frequency. The method assumes that the structure is linear, the excitation is ambient, and the damping of the structure is light with well-separated modes (Felber 1993). The natural frequencies of the structure are identified from the peaks of normalized cross power spectral densities (PSD)s, and the mode shapes are found from the ratio of cross PSDs. Although the theory behind peak-picking may be comprehensive, this method is highly practical and user-friendly. During the process, peaks in the PSDs are selected based on the physical understanding. This feature allows the method to be understood by a group of variety background. For this reason, this method has been chosen in this study.

To obtain accurate results in the peak-picking method, both low noise levels in the signals and clear, distinctive peaks are essential. Low accuracy in the lower frequencies in the MEMS based low-cost accelerometers may harm the use of the methods for civil structures, where the fundamental frequencies are usually low (Su *et al*. 2010, Nagayama *et al*. 2005). To enhance the accuracy, Nagayama *et al*. (2010), suggested using limited number of high-sensitivity acceleration for the reference signals when calculating cross-PSDs. Such multi-metric network offers cost-effective extraction of the system identification with increased accuracy for peak-picking method.

3.2 Modal identification

In this section, system identification of the bridge using a set of signals from the acceleration network is presented. In the modal analyses, peak-picking and NExT ERA methods are employed to find fundamental characteristics of the bridge. Used measurements are transient responses of the bridge after Amtrak crossed the bridge. This signal is preferred over other records, such as under or after a freight train, because the effect of Amtrak increasing the weight of the bridge is negligible due to its light weight and fast speed (over 80 km/h). Fig. 4(a) shows vertical responses from the West side of WSSs, which are sampled at 25 Hz. Although the vibration level of the measurements are small, due to light damping of the structure, the bridge experienced more than 40 seconds of gradual decrease of the response. Fig. 4(b) shows auto spectral density calculated using Hanning Window with 1024 NFFT. The line with ‘+’ marker corresponds to the lateral vibration collected from a sensor at D-W (see Fig. 2). This SHM-H sensor shows apparently lower noise level within the frequency zone of interest with clear peaks at fundamental frequencies of the bridge. To benefit the modal analyses by reducing the total noise level in the network, auto spectral density of D-W sensor was used as the reference signal in the identification of the lateral mode shapes.

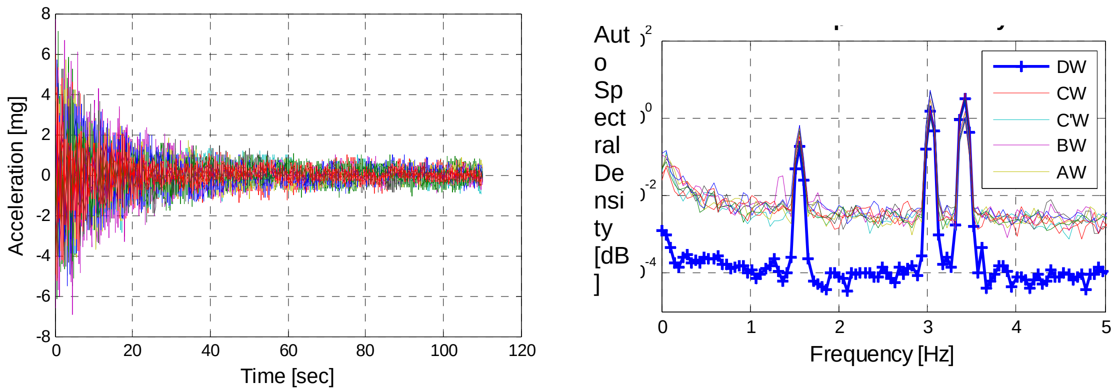

(a) Time history (b)Auto spectral density.

Fig. 4 Vertical responses measured from the West side of the truss bridge

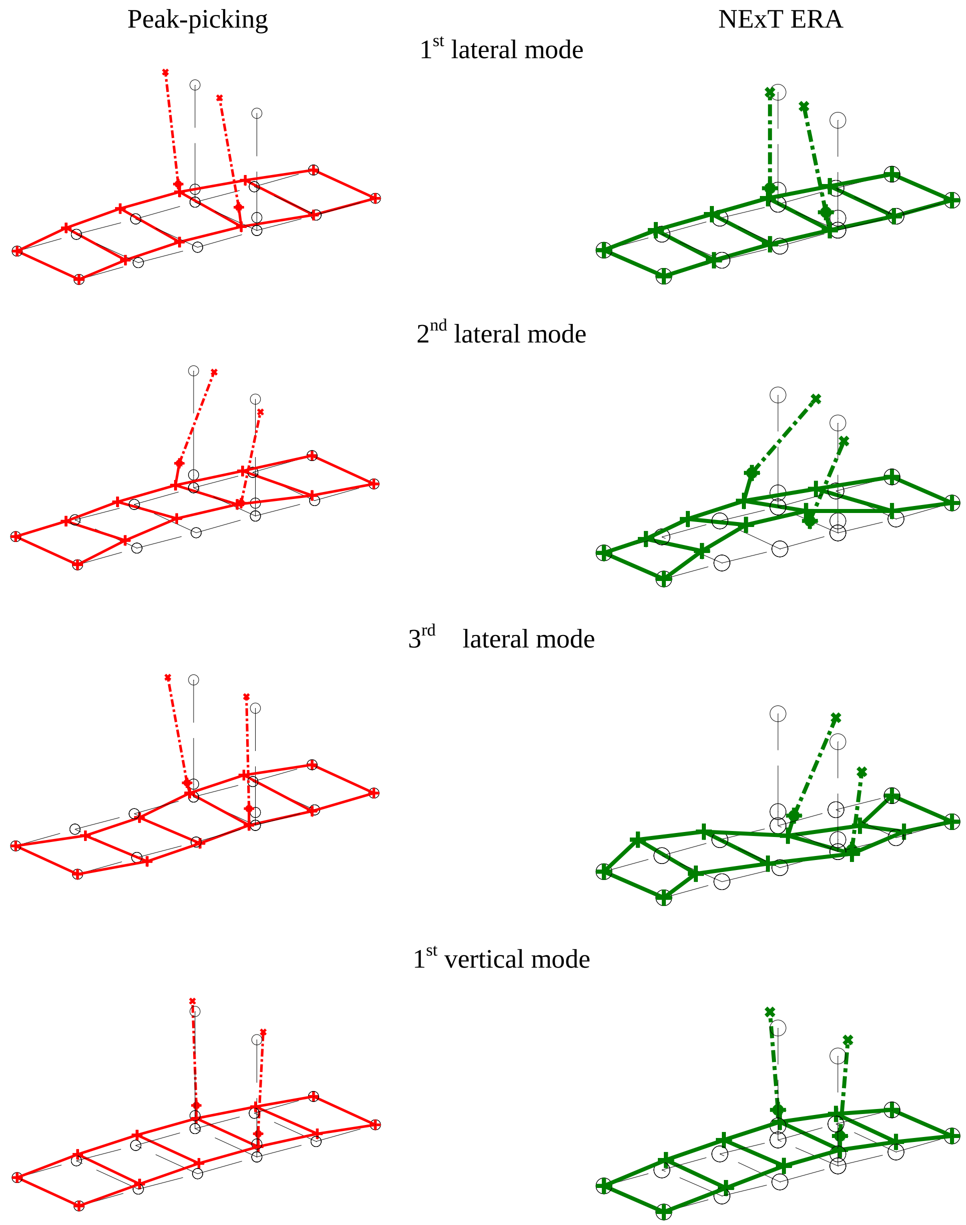

Fig. 5 Mode shape comparison, Peak-picking and ERA comparison

Fig. 5 compares mode shapes from peak-picking and NExT ERA methods. In the peak-picking method, the peaks are manually selected from auto spectral density. For visualization purposes and to ease the task of picking peaks from the reference auto spectral density, signals are regulated and divided by the minimum noise level. As a result, they end up having the same noise level. By doing so, the reference signal shows the highest amplitude at the pick. Then, mode shapes are calculated at the selected frequencies by using the reference auto spectral density.

Table 1 Natural frequency comparisons; Peak-picking and NExT ERA comparison

Candidate Modes	Peak-picking [Hz] (Error [%]†)	NExT ERA [Hz]<EMAC>
1st lateral	1.542(0.065)	1.541<99.84>
2nd lateral	3.014(0.660)	3.034<99.99>
3rd lateral	3.390(0.732)	3.415<99.99>
1st vertical	3.592(1.756)	3.530<99.92>

†Absolute error: A (|A-B|/B), where A = Peak-picking; B = NExT ERA

In NExT ERA method, on the other hand, the cross correlation matrix based on the selected reference signals is calculated. Then, the system properties are extracted by employing the eigenvalue problem for the system realization matrix solved through the decomposed of the Hankel matrix (Juang and Pappa 1986, James *et al*. 1993). To select only meaningful modes, those with high Extended Modal Amplitude Coherence (EMAC) are chosen (Pappa *et al*. 1993). Table 1 summarizes differences between natural frequencies identified in two methods. Having less than 2% differences in the results, peak-picking method can be considered as reliable and accurate as NExT ERA method while preserving simplicity and user-friendliness.

4. Finite element model

For several decades, FE models have been widely used for simulating and assessing the structural behavior under arbitrary structural conditions. To build a model with such capability, a preliminary analytical FE model is developed in Matlab® using the shop drawings from CN's construction records. The model contains 345 nodes and 724 elements. The boundary conditions at the North and South bearing supports are pin and expandable, respectively. Nodes are frame connected, which can transfer rotational moments to adjacent elements. The initial FE model developed based on the drawing is shown in Fig. 6. Table 2 summarizes first four modes identified using this model.

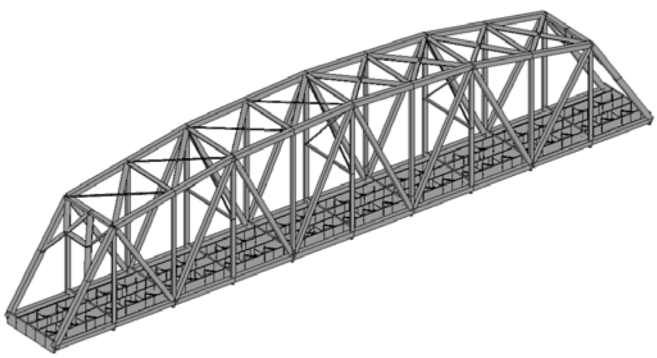

Fig. 6 The bridge model

Table 2 Natural frequency comparisons between peak-picking and initial FE model

Candidate Modes	Peak-picking [Hz]	Initial FE model [Hz]	
		Mode [Hz]	Error [%][†]
1st lateral	1.542	1.819	17.96
2nd lateral	3.014	2.875	4.612
3rd lateral	3.390	3.774	11.33
1st vertical	3.592	4.025	12.05

[†](|A-B|/A), where A = Peak-picking; B = FE model


(a) Track system, rail, and fastening

(b) Lacings

Fig. 7 Bridge additional mass components

As can be seen from Table 2, the initial FE model does not fully represent the current physical state of the bridge. Part of reasons are:

- The initial model represented only the truss structure and did not include track system.
- Most main sections are built-up sections with holes on each side as shown in Fig. 7. However, those details were excluded to keep the model simple.
- For brevity of the modeling, all floor systems shared the same neutral axes, while they were in fact located at different levels.
- The boundary conditions and joints between elements were modeled as shown in the drawings, but those may have been changed from the time of original construction.

Thus, the model needs to be updated to better represent the bridge. For example, the shop drawing indicated that the total weight of the bridge is approximately 11,120 kN (2500 kips), which was larger than the preliminary FE model. As discussed earlier, these differences arise from neglecting track system, rail and fastening, lacings and other utilities (see Figs. 7(a) and 7(b)). For example, the dead load of rail and fastening elements per track are approximately 889.64 N per meter (200 lb_F per feet, Unsworth 2010). To accommodate the omitted mass, additional mass is distributed and lumped on the floor nodes. After updating the mass, the mass ratio between the bridge and total train represents the actual ratio; a standard Amtrak train composed of one engine and seven cars is about 20% of the bridge weight.

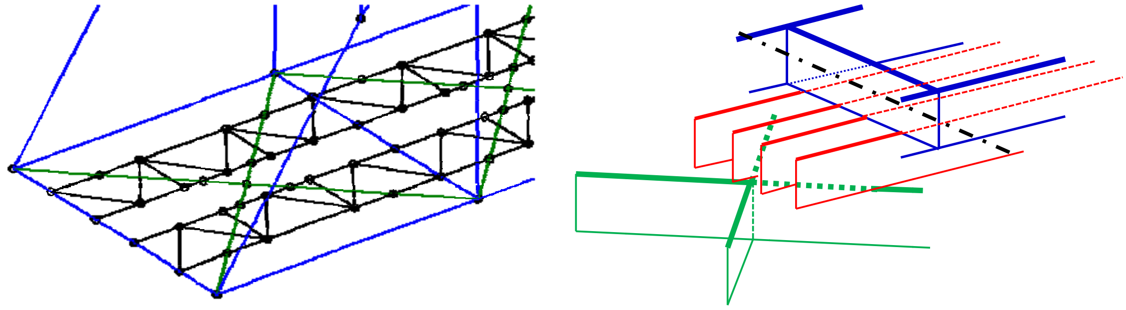

Fig. 8 Floor system in detail

The floor system of the bridge is rigid because three layers are acting as one unit: the lower chords, the floor beams, and the stringers and bottom lateral bracings. To capture such rigidity, the moment of inertias for those layers is calculated about one reference axis, which is the center of lower chords (see Fig. 8). This calculation simplifies the complexity of modeling three layers for the floor system. The following modal analysis of the FE model with updated mass and floor system validates that the model well represents the bridge.

Identified first four modes from the updated FE model show the fundamental dynamic characteristics of the bridge. The first, second and third lateral modes are at 1.551 Hz, 3.054 Hz, and 3.242 Hz, respectively. The first vertical mode is at 3.567 Hz. The next section will show that the model has reached sufficient level of accuracy. Therefore, employing sophisticated model updating techniques such as generic algorithm would be redundant.

5. Model validation

5.1 Model validation with global responses

To validate that the FE model can represent the bridge performance in global sense, numerically identified natural frequencies and their mode shapes are compared with experimentally identified results under transient responses after Amtrak, as shown in Fig. 9. For efficient visualization, the first column shows the deformed mode shapes of global nodes. To reduce the spatial aliasing, the second column shows the deformed mode shapes using the deformations only at the locations of the WSSs. The mode shapes in the third column are experimentally identified, with linear extension of the upper chords where the higher sensors are located 2.1 m higher from the bottom chord (dashed-line in the third column). The mode shapes in the FE model agree well with the mode shapes obtained experimentally.

Table 3 summarizes the frequencies at each mode. The model shows a good agreement with the experimentally derived data, with an error of less than 5% for all modes. In addition, numerically obtained mode shapes are correlated with the experimental ones using the modal assurance criterion (MAC). MAC values obtained between the first four mode shapes are shown in Table 3. All modes show MAC values over 90%, indicating that the model well represents the bridge in a global sense. The following section will demonstrate the accuracy of the model in simulating local responses of the bridge, which is important for assessing the state of the bridge under an arbitrary trainload.

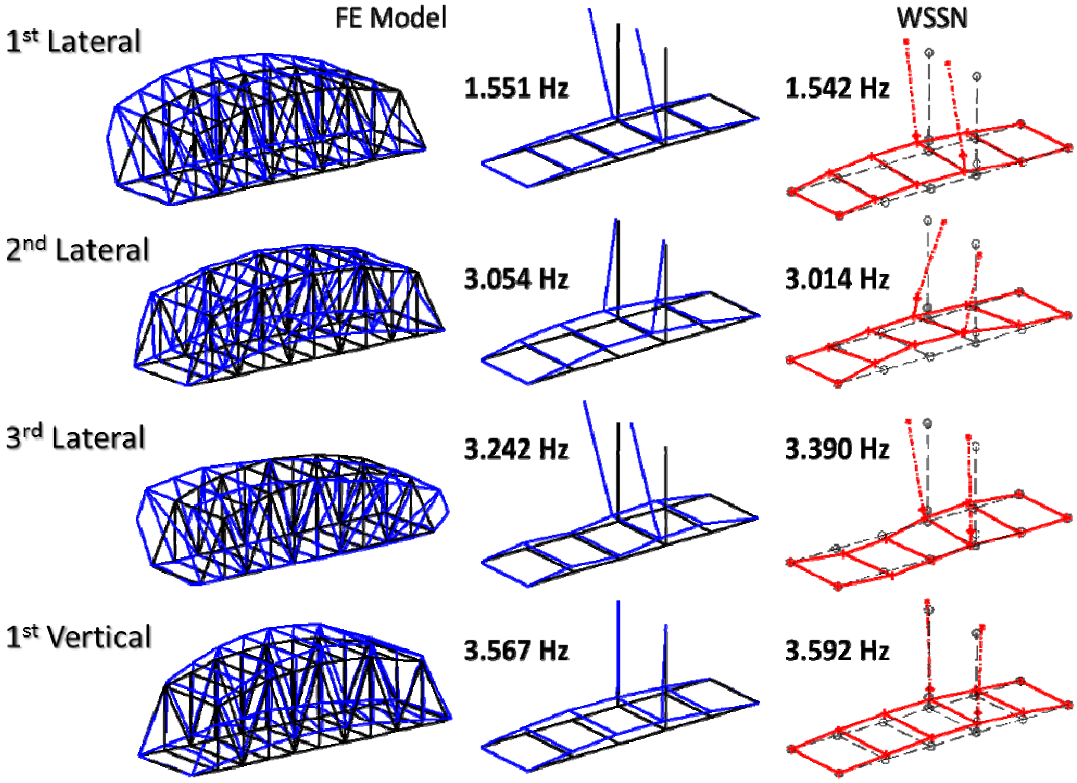

Fig. 9 Modal analysis comparison with FE model

Table 3 Mode comparison

	Peak-picking: WSSN [Hz]	FE model		
		[Hz]	(Error [%])†	MAC [%]
1st Lateral	1.542	1.551	(0.584)	91.34
2nd Lateral	3.014	3.054	(1.327)	94.17
3rd Lateral	3.390	3.242	(4.366)	90.97
1st Vertical	3.592	3.567	(0.696)	98.38

†Absolute error: A (|A-B|/B), where A = Peak-picking; B = FE model

5.2 Model validation using local responses

This section presents the model validation using local responses of the bridge. Here, strain response from SHM-S sensor (Fig. 2) under a train of known mass is used. Collaborating with CN, a test car (Fig. 10) ran over the bridge while the SHM system collected the strain response. During the experiments, the test train ran on CN1 track multiple times with varying speeds (from 8 km/h to 80 km/h) and directions (in the North bound (NB) and the South bound (SB)). The length of the test train was 120 m with total weight of 7,340 kN. A locomotive and seven cars had different wheel loads profile varying from 73 kN/wheel to 143 kN/wheel. Although this tests were performed under a controlled test, for a revenue train, wheel loads and train speed information can be retrieved from a train manifest.

Fig. 11 shows an example of the instrumented member strain collected at 280 Hz when the test train crossed the bridge. The measurements at speeds varying from 8 km/h to 80 km/h indicate that the dynamic component is relatively small and static component dominates the signature of the member strain. Regardless of speeds, the member experiences both compression and tension as the train passes, with the maximum compression near 50 με and the maximum tension around the 60 με.

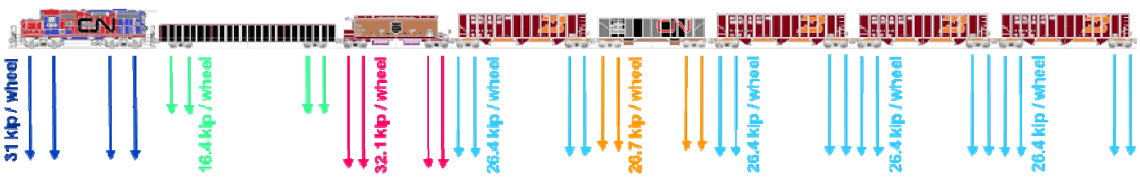

Fig. 10 Test train wheel loads scheme

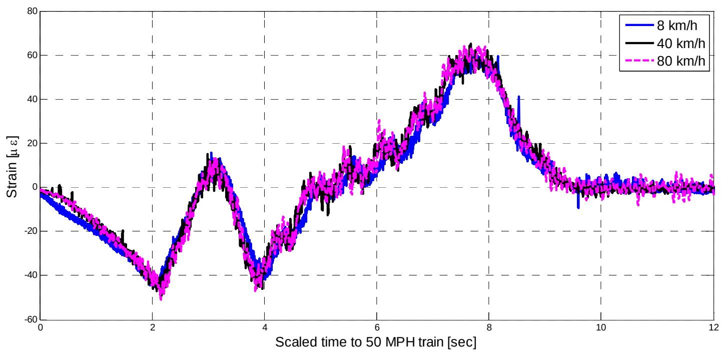

Fig. 11 An instrumented member strain under the test train at speeds 8, 40, and 80 km/h

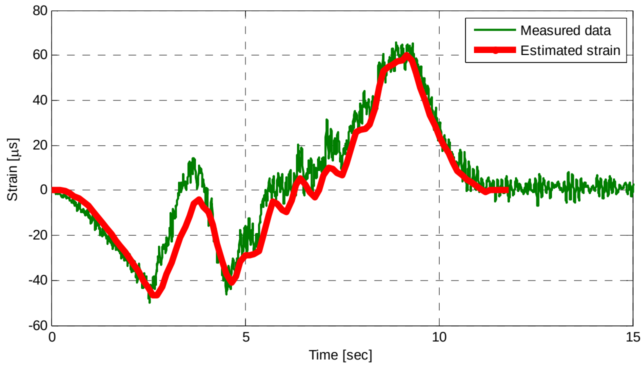

Fig. 12 Member strain comparison with field measured data and static estimation

Static analysis is used to estimate the strain from the FE model, observing that the dynamic component in the measured data is not significant. In the analysis, the location of the train is determined at each time step. For example, the first time step assumes that the head of train is at the South entrance of the bridge. Then, the wheel loads are distributed at the nodal points of the bridge model as a series of point loads. After obtaining the member strain at the time step, train location is re-determined assuming the train headed the North with small amount. This sequence is iterated until the train fully exits the North end of the bridge. Fig. 12 shows the comparison of static estimation and field measurements. Overall, 200 iterative time steps were used in the analysis. The obtained strain well captures the maximum compression and tension that the member actually experienced. For practical purposes, obtaining those maximum values are usually the ones of most concern, exerting that the proposed approach is adequate. Subsequently, one can conclude that this approach has potentials to be expanded for estimating bridge responses under arbitrary revenue train with given wheel loads. However, due to dynamic interactions between the vehicle, track, and the bridge, some discrepancies between the estimated strain and measured strain are observed around 4 seconds. Thus, a further evolution of the model to include dynamic analyses of the model needs to be performed.

6. Conclusions

This paper demonstrated an approach to system identification and dynamic testing with the goal of understanding the in-service response of railroad bridges. High fidelity data has been obtained from a structural health monitoring (SHM) system using wireless smart sensors (WSSs). The final deployment of the system has considered obtaining asymmetric responses and reducing physical aliasing, while retaining cost-effectiveness. Then, a finite element model has been developed based on the shop drawings. Because the initial model did not well represent the bridge, selected parameters are updated. The final model was validated using both global and local responses of the field-measured data; acceleration responses of the bridge validated the global features of the bridge and a member strain demonstrated that the model could well capture the local responses of the bridge. The static analysis proposed in this paper indicated that the approach could well capture the maximum compression and tension of the selected member, while dynamic approach is still required if reconstructing accurate strain history is of concern. Nonetheless, with this accurately calibrate model and static analysis, a sufficient level of assessment about the bridge can be made. For example, arbitrary wheel loads and train topologies can be determined from the model simulation and allowable member strain. This result showed the potential of turning a model from explanatory in nature to having powerful predictive capabilities that can help assessing the state of the railroad bridge.

Acknowledgements

This study is supported by the Federal Railroad Administration under the BAA 2010-1 project (Cameron Stuart, program manager). In addition, the technical support from CN is greatly appreciated.

References

Association of American Railroads (2012), An Overview of America’s Freight RailroadsExternal Link.

Ahmadi, H.R. and Daneshjoo, F. (2012), “A harmonic vibration, output only and time-frequency representation based method for damage detection in Concrete piers of complex bridges”, *Int. J. Civil Struct. Eng.*, **2**(3), 987-1002 .

Brenner, B., Bell, E., Sanayei, M., Pheifer, E., Durack, W., Fay, S. and Thorndike, L. (2010), “Structural modeling, instrumentation, and load testing of the Tobin Memorial Bridge in Boston, Massachusetts”, *Proceedings of the 2010 Structures Congress*, Orando, Florida, May.

Brincker, R., Zhang, L. and Andersen, P. (2001), “Modal identification of output-only systems using frequency domain decomposition”, *Smart Mater. Struct.*, **10**(3), 441-445.

Brownjohn, J. (2003), “Ambient vibration studies for system identification of tall buildings”, *Earthq. Eng. Struct. D.*, **32**(1), 71-95.

Brownjohn, J.M. and Xia, P.Q. (2000), “Dynamic assessment of curved cable-stayed bridge by model updating”, *J. Struct. Eng.- ASCE*, **126**(2), 252-260.

Catbas, F.N., Ciloglu, S.K., Hasancebi, O., Grimmelsman, K. and Aktan, A.E. (2007), “Limitations in structural identification of large constructed structures”, *J. Struct. Eng. - ASCE*, **133**(8), 1051-1066.

Catbas, F.N., Susoy, M. and Frangopol, D.M. (2008), “Structural health monitoring and reliability estimation: Long span truss bridge application with environmental monitoring data”, *Eng. Struct.*, **30**(9), 2347-2359.

Cho, S., Giles, R.K. and Spencer, B.F. (2014), “System identification of a historic swing truss bridge using a wireless sensor network employing orientation correction”, *Struct. Control Health. Monit.*, **22**(2), 255-272.

Crossbow Technology Inc. (2009), Imote2 - High-performance Wireless Sensor Network Node, Available at http://www.xbow.com/Products/Product_pdf_files/Wireless_pdf/Imote2_Datasheet.pdf

Deng, L. and Cai, C. (2009), “Bridge model updating using response surface method and genetic algorithm”, *J. Bridge Eng.*, **15**(5), 553-564.

Federal Railroad Administration (2010), National Rail Plan Progress Report.

Felber, A.J. (1993), *Development of a hybrid bridge evaluation system*, Ph.D. Dissertation, University of British Columbia, British Columbia.

Government Accountability Office (GAO; 2007), Railroad Bridges and Tunnels: Federal Role in Providing Safety Oversight and Freight Infrastructure Investment Could Be Better Targeted. GAO-07-770, August 6, 2007.

Giles, R., Kim, R., Sweeney, S., Spencer, B., Bergman, L., Shield, C. and Olson, S. (2014), "Multimetric monitoring of a historic swing bridge", *Bridges*, **10**, 9780784412374.014.

Giles, R., Kim, R., Spencer Jr, B.F., Bergman, L.A., Shield, C.K. and Sweeney, S.C. (2011), "Structural health indices for steel truss bridges",*Conference Proceedings of the Society for Experimental Mechanics Series*, Jacksonville, Florida, January.

Jaishi, B. and Ren, W.X. (2005), "Structural finite element model updating using ambient vibration test results", *J. Struct. Eng.- ASCE*, **131**(4), 617-628.

James III, G.H., Carne, T.G. and Lauffer, J.P. (1993), *The natural excitation technique (NExT) for modal parameter extraction from operating wind turbines*, NASA STI/Recon Technical Report N, **93**, 28603.

Jo, H., Sim, S.H., Mechitov, K.A., Kim, R., Li, J., Moinzadeh, P., Spencer Jr, B., Park, J.W., Cho, S. and Jung, H.J. (2011), "Hybrid wireless smart sensor network for full-scale structural health monitoring of a cable-stayed bridge", *Proceedings of the SPIE Smart Structures/NDE Conference*, San Diego. California, March.

Jo, H., Sim, S.H., Nagayama, T. and Spencer Jr, B. (2011), "Development and application of high-sensitivity wireless smart sensors for decentralized stochastic modal identification", *J. Eng. Mech. - ASCE*, **138**(6), 683-694.

Juang, J.N. and Pappa, R.S. (1986), "Effects of noise on modal parameters identified by the eigensystem realization algorithm", *J. Guid. Control Dynam.*, **9**(3), 294-303.

Juang, J.N. and Pappa, R.S. (1985), "An eigensystem realization algorithm for modal parameter identification and model reduction", *J. Guid. Control Dynam.*, **8**(5), 620-627.

Morassi, A. and Tonon, S. (2008), "Dynamic testing for structural identification of a bridge", *J. Bridge Eng.*, **13**(6), 573-585.

Nagayama, T., Abe, M., Fujino, Y. and Ikeda, K. (2005), "Structural identification of a nonproportionally damped system and its application to a full-scale suspension bridge", *J. Struct. Eng.- ASCE*, **131**(10), 1536-1545.

Nagayama, T., Ushita, M., Fujino, Y., Ieiri, M. and Makihata, N. (2010), "The combined use of low-cost smart sensors and high accuracy sensors to apprehend structural dynamic behavior", *Proceedings of the SPIE Smart Structures/NDE Conference*, San Diego. California, March.

Pappa, R.S., Elliott, K.B. and Schenk, A. (1993), "Consistent-mode indicator for the eigensystem realization algorithm", *J. Guid. Control Dynam*, **16**(5), 852-858.

Rice, J.A., Mechitov, K., Sim, S.H., Nagayama, T., Jang, S., Kim, R., Spencer Jr, B.F., Agha, G. and Fujino, Y. (2010), "Flexible smart sensor framework for autonomous structural health monitoring", *Smart Struct. Syst*, **6**(5-6), 423-438.

Rice, J.A. and Spencer Jr, B. (2008), "Structural health monitoring sensor development for the Imote2 platform", *Proceedings of the 15th International Symposium on: Smart Structures and Materials & Nondestructive Evaluation and Health Monitoring*, San Diego, California, March.

Su, D., Fujino, Y., Nagayama, T., Hernandez Jr, J.Y. and Seki, M. (2010), "Vibration of reinforced concrete viaducts under high-speed train passage: measurement and prediction including train–viaduct interaction", *Struc.Infrastruct. E.*, **6**(5), 621-633.

Unsworth, J.F. (2010), *Design of modern steel railway bridges Editioned*., CRC Press.

Van Damme, S., Boons, B., Vlekken, J., Bentell, J. and Vermeiren, J. (2007), "Dynamic fiber optic strain measurements and aliasing suppression with a PDA-based spectrometer", *Meas. Sci. Technol.*, **18**(10), 3263-3266.